Published in Journal of Optics A: Pure and Applied Optics 10, issue 6, 921-931, 2004
which should be used for any reference to this work

Rigorous diffraction theory applied to the analysis of the optical force on elliptical nano- and micro-cylinders

Carsten Rockstuhl[1] **and Hans Peter Herzig**

University of Neuchâtel, Institute of Microtechnology, Rue A-L Breguet 2, CH-2000 Neuchâtel, Switzerland
E-mail: carsten.rockstuhl@unine.ch

Abstract
Illumination of nano- and micro-particles with a highly focused laser beam will exert a force on them that depends on different parameters, such as the particle size, refractive index and beam waist. In this paper rigorous diffraction theories are used to calculate the force on elliptically shaped dielectric cylinders in three different size regimes. We analyse the conditions for which the particles are attracted or repelled from the optical axis as a function of the geometry. Such a shape dependent response to optical wave-fields could be used to sort particles.

Keywords: rigorous diffraction theory, MMP, optical force, optical tweezer, trapping

1. Introduction

Based on the pioneering work of Ashkin in the early seventies [1, 2], it is known that by illuminating dielectric micro- and nano-particles with laser beams a force is applied to the particles due to the exchange of momentum between the photons and the object [3]. Different interaction regimes can be distinguished, depending on the size and the shape of the particles, the parameters that characterize the illuminating beam and the contrast of the refractive index (defined as n_i/n_a, with n_i the refractive index of the object and n_a the index of the surrounding medium) [4]. It becomes possible to attract and accelerate particles along the optical axis in the propagation direction of the illuminating laser beam for particles that have a higher index of refraction than the surrounding medium [5]. The particles are repelled from the optical axis if the index contrast is smaller than unity [6]. For particles much smaller than the wavelength, it is possible to find points in space where all the forces that act on the particle are equal and the object is stably trapped in three dimensions [7]. Such optical tweezers have gained a lot of interest in the past due to their large range of possible applications, both in fundamental as well as in applied sciences. Two examples are the levitation of particles [8] or near-field scanning optical microscopy [9].

For a qualitative description of how optical tweezers work, two different approaches are usually used which apply in different size regimes. The ray-optics model is used to explain the behaviour of optical tweezers if the particle size is much larger than the wavelength. The beam is treated as a superposition of rays and the two refractions when a ray enters and exits the particle are modelled using Snell's law. Each ray undergoes a change in momentum between the incoming and outgoing ray. Due to conservation laws, the momentum in a system remains invariant, so the transfer of momentum between ray and particle can be calculated for each ray that is refracted. Summing up the momenta will result in a net force, which will accelerate the particle [6].

For particles much smaller than the wavelength, such a ray-optics model does not apply. For these particles a dipole approximation can be used for describing the light–particle interaction to characterize the scattering properties in a simplified manner. The object is considered as an emitting

[1] Author to whom any correspondence should be addressed.

dipole and the force that acts on the particle can be decomposed into a scattering and a gradient force [10].

If the size of the particle is comparable to the wavelength, neither approximation can be used and instead the problem must be solved rigorously in two steps. In the first step, the diffraction problem is solved and the field around the particle is calculated rigorously. The force acting on the particle can be determined in the second computational step by applying Maxwell's stress tensor [11]. A simple and elegant way to find the field around spherical objects is the use of the generalized Lorenz–Mie theory (GLMT) [12], which describes in its original formulation strictly the interaction of an arbitrary shaped beam with a homogenous sphere. The theory makes use of an expansion of the field components using scalar potentials and a separation of variables in the coordinate system associated with the particle [13]. Consequently, this size regime is often called the Mie domain [14]. The theory has been extended to other geometries, such as layered spheres [15], cylindrical objects [16] and elliptical cylindrical objects [17]. In the past the theory was also applied to calculate the optical force on spheres [18] and more recently by Lock [19, 20]. Force and torque calculations on other geometries such as multilayered spheres [21] have been also reported.

For non-spherical objects the diffraction problem can be solved with various methods. In the past Nieminen *et al* applied the T-matrix approach to the problem and calculated the force on some non-spherical objects [11, 22]. Nieto-Vesperinas *et al* demonstrated that the coupled dipole method (CDM) can be used for this problem [23] and analysed the force on circular cylinders above surfaces.

In this paper we will apply the multiple multipole method [26] to analyse the force exerted on cylindrical circular and elliptical objects for different size domains and for different index contrasts as a function of the axis ratio. Such a rigorous treatment for non-circular particles was mainly restricted in the past to specific calculations for a set of parameters that corresponds to an experimental situation. No comprehensive rigorous analysis of the force on particles with a non-circular geometrical cross section has been performed so far. In this paper, we will present this rigorous analysis and show explicitly the transition of the force between the different size regimes. We will restrict ourselves to two-dimensional objects that are of infinite extent in the third dimension. All of the main physical aspects are included in this model, which allows us to analyse the behaviour of these particles without any approximation.

2. Calculating the force on arbitrarily shaped particles

To calculate the force that acts on arbitrarily shaped micro- and nano-particles the computational procedure consists of two steps. In the first step the electro-magnetic field distribution along the surface of the object must be solved rigorously.

For simplicity and because the force will be calculated in various positions relative to the waist of a given illuminating laser beam propagating in the positive z-direction, the most common approach is to decompose the illuminating beam into a plane wave spectrum and calculate the field distribution for each illumination direction separately. For a numerical description the spectrum is discrete, with a finite number of plane waves, which will introduce a periodicity of the illuminating beam of Λ. If the particle is positioned at a point (x, z) relative to the centre of the waist of the beam, the complex amplitude of the mth order illumination plane wave is given by [27]

$$A_m = \frac{\mathrm{e}^{-\mathrm{i}\sqrt{(\frac{2\pi}{\lambda})^2-(m\frac{2\pi}{\Lambda})^2}z}}{\Lambda}\int_{-\frac{\Lambda}{2}}^{\frac{\Lambda}{2}} a_{\mathrm{Inc}}(x)\mathrm{e}^{-\mathrm{i}m\frac{2\pi}{\Lambda}x}\,\mathrm{d}x, \qquad (1)$$

with $a_{\mathrm{Inc}}(x)$ being the amplitude distribution in the waist; Λ is the assumed periodicity of the illuminating wave-field that has to be chosen large enough. m is the diffraction order. $a_{\mathrm{Inc}}(x)$ for a Gaussian beam in the waist is given by

$$a_{\mathrm{Inc}}(x) = E_0\mathrm{e}^{-\left(\frac{x}{\omega}\right)^2}, \qquad (2)$$

with E_0 the beam amplitude and ω the waist. However, the final beam used in the calculation for the illumination is not given by this equation, as a focused Gaussian beam does not satisfy equation (2). The angular spectrum of the illuminating beam is truncated, such that only the propagating waves will interact with the sphere. The evanescent waves of the angular spectrum will not contribute. Neglecting the effects of a necessary high NA system to obtain a highly focused laser beam, the illuminating beam as described by equations (2) and (1) can be generated by a classical far-field lens system. We used $\Lambda = 20\lambda$, which will give 41 propagating orders in air. To solve the interaction of a plane wave with cylindrical objects, the multiple multipole method (MMP) is used [32, 26, 31]. The MMP is a semi-analytical method, in which the description of the electromagnetic field in regions with a homogenous dielectric constant uses known analytical solutions of the wave equation. The field is written as a superposition of multipoles emitting from different spatial positions. The multipoles are Hankel functions of the first order and 75 multipoles were used for convergence of the numerical results. The surface was sampled using 500 points. If the fields across the surface of the particle are calculated for each propagation direction, the entire field at an arbitrary point in the space is given by a superposition of the plane wave response multiplied by the appropriate amplitude coefficient A_m.

Once the field is known, the second step involves the application of Maxwell's stress tensor to find the force on the particle [28, 29]. At optical frequencies only the time average of the electromagnetic force is observed. For a particle embedded in an isotropic medium the force is calculated as [30]

$$\langle\vec{F}\rangle = \int_S \left\{\frac{\epsilon}{2}\mathrm{Re}[(\vec{E}\cdot\vec{n})\vec{E}^\star] - \frac{\epsilon}{4}(\vec{E}\cdot\vec{E}^\star)\vec{n} + \frac{\mu}{2}\mathrm{Re}[(\vec{H}\cdot\vec{n})\vec{H}^\star] - \frac{\mu}{4}(\vec{H}\cdot\vec{H}^\star)\vec{n}\right\}\mathrm{d}l' \qquad (3)$$

with S being the surface of the particle and $\vec{n}$ the normal to the surface pointing outward.

To ensure the correct implementation of our algorithm, we have first compared it with results published in the literature by Chaumet *et al* [23]. Excellent agreement was found for both polarizations for the force acting on a 10 nm glass cylinder. In addition we compared results for a dielectric cylinder with different radii calculated with Lorenz–Mie

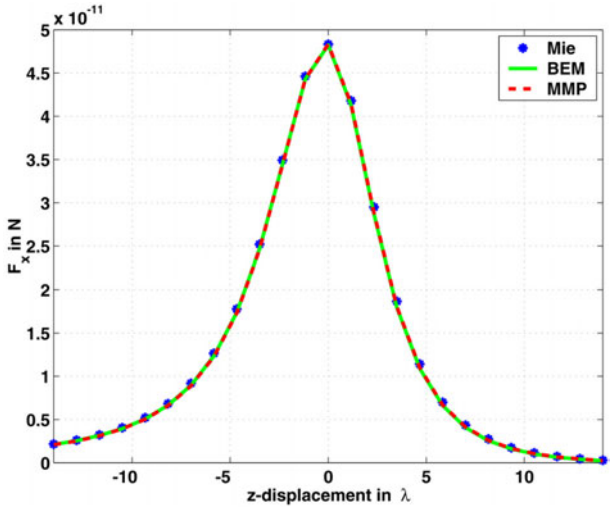

Figure 1. Transverse force on a circular cylinder calculated with three different techniques (parameters are given in the text).

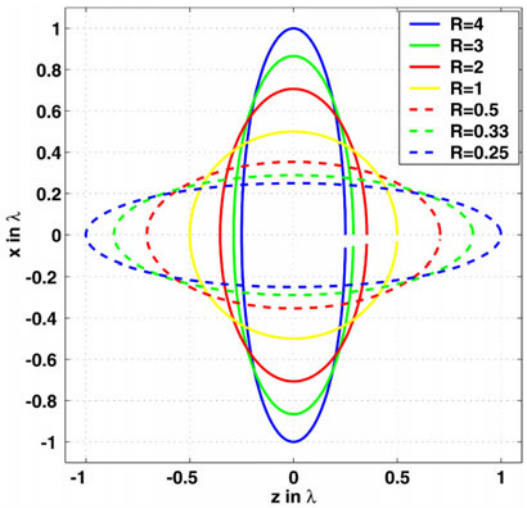

Figure 2. Geometry of the elliptical particles used in the simulation.

theory [33], with the MMP and also with the boundary element method (BEM) [24, 25]. In all cases the results agree very well. As an example we show in figure 1 the transverse force acting on a cylinder with $r = 0.5\lambda$ and $n = 1.5$ evaluated along the z-axis at $x = -0.44\lambda$. The illuminating beam was a Gaussian one with a waist of $\omega = \lambda$. The refractive index of the surrounding medium was air. All three methods give the same result. An interpretation of the results is given in the next section, where we analyse the force exerted on dielectric cylinders in air by a Gaussian beam.

3. Large dielectric particles in air

In this section we analyse the force on elliptical particles made of glass ($n_i = 1.5$) in air as a function of the elongation if their size is comparable to the wavelength. Figure 2 shows the geometry of the particles used for the simulation as a function of the axis ratio R. The axis ratio is defined as $R = \frac{r_2}{r_1}$. The radius r_1 is the radius of the elliptical cylinder in the z-direction, the direction of propagation of the laser beam. They all have an equal area and seven different ellipticities are considered. The three elongations are chosen by multiplying the reference radius r_{Ref} by $\sqrt{2}$, $\sqrt{3}$ and $\sqrt{4}$. To keep the area constant in each case, the orthogonal radius is divided by the same factor. The two different elongation directions are transversal (perpendicular to the optical axis, with the radius r_1 being the reference radius multiplied by a factor smaller than unity) and longitudinal (parallel to the optical axis, the radius r_1 being the reference radius multiplied by a factor larger than unity).

In figures 3(a) and (b) the longitudinal force that acts on the particles along the optical axis is shown for a cylinder with a reference radius of $r_{\mathrm{Ref}} = 0.5\lambda$ as a function of the elongation for TE polarization and for TM polarization. The particles are illuminated with a Gaussian beam. For all of our simulations, if not stated otherwise, we have chosen a waist ω equal to the wavelength and the amplitude of the illuminating Gaussian beam was chosen to be 6.9 V m^{-1} that is the corresponding amplitude of the three-dimensional beam

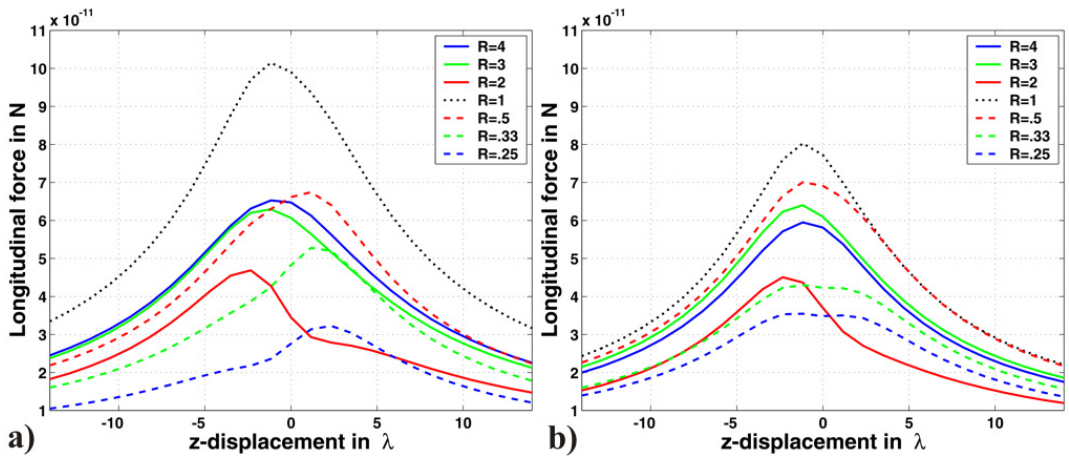

Figure 3. Longitudinal force on a dielectric elliptical cylinder on the axis with $r_{\mathrm{Ref}} = 0.5\lambda$ assuming (a) a TE-polarized and (b) a TM-polarized Gaussian beam for illumination.

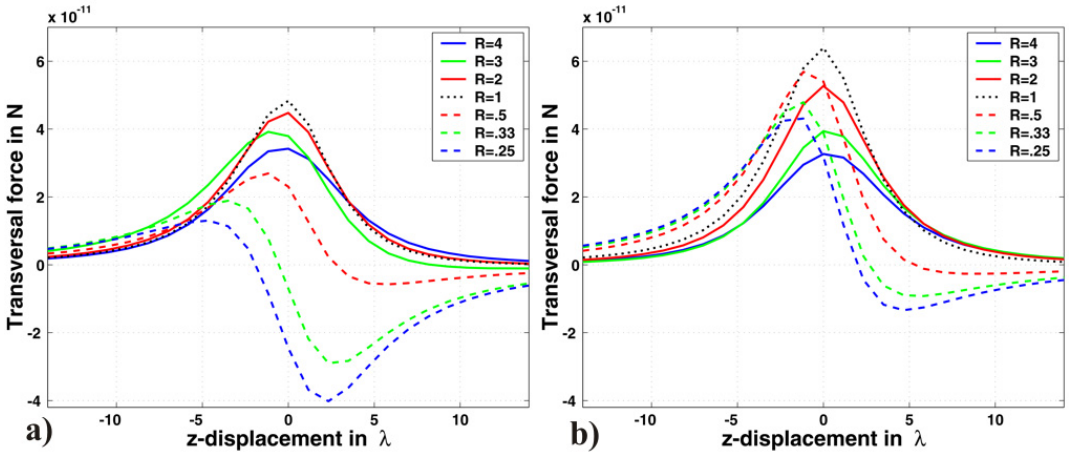

Figure 4. Transversal force along $x = -0.44\lambda$ on a dielectric elliptical cylinder with $r_{\mathrm{Ref}} = 0.5\lambda$, assuming (a) a TE-polarized and (b) a TM-polarized Gaussian beam for illumination.

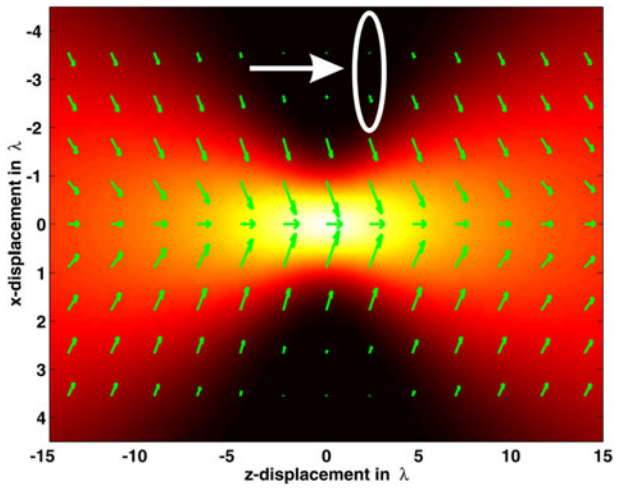

Figure 5. Force acting on a dielectric elliptical cylinder of transversal elongation ($r_1 = \frac{0.5}{\sqrt{4}}\lambda$).

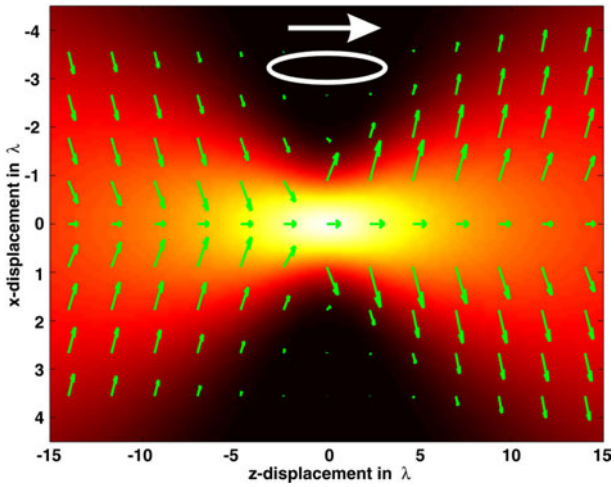

Figure 6. Force acting on a dielectric elliptical cylinder of longitudinal elongation ($r_1 = 0.5\sqrt{4}\lambda$).

with a power of 100 mW. First of all, no pronounced difference exists between TE and TM polarization. It can be seen that the force always has a maximum close to the waist of the laser beam and the force pushes the particle along the optical axis, it is always positive. The strength of the force is in the range of tens of piconewtons. No uniform trend can be seen in the dependence between the elongation and the strength of the force, due to multiple reflections of the light within the structure. Such a trend will appear if the particles are smaller, because the light that encounters the multiple reflections suffers from substantially smaller phase delay. For the particles with a reference radius of half of the wavelength, the force is strongest for the circular cylinder independent of the polarization.

The transversal force at a small distance from the optical axis (the value for the distance was chosen somewhat arbitrary to be $x = -0.44\lambda$) is shown for the particles in figure 4(a) for TE and 4(b) for TM polarization. Again, no pronounced difference can be seen for the two polarizations. A positive force means that the particles are attracted towards the optical axis, a negative one corresponds to a repulsion. It can be seen in both figures that particles elongated perpendicular to the optical axis are always attracted, while particles elongated in the opposite direction are attracted before and repelled approximately after the waist. The most elongated of these particles are already repelled somewhat before the waist. The effect is more pronounced using TE-polarized light.

The entire force distribution for the two most elongated particles (one transverse with $r_1 = \frac{0.5\lambda}{\sqrt{4}}$ and one longitudinal with $r_1 = 0.5\lambda\sqrt{4}$) assuming TE polarization is shown in figures 5 and 6. The length of the arrows is not linearly proportional to the force in order to emphasize the direction of the force. The amplitude of the illumination beam is also shown in the figures and it propagates along the positive z-axis and in the insets of the figures the geometry of the particle with respect to the illumination direction is shown. Obviously the effect of attraction or repulsion is not restricted to a region close to the optical axis. Particles elongated parallel to the optical axis are repelled if they are located behind the beam waist. For an explanation of this effect we have performed simulations using a finite difference time domain (FDTD) [34]. Such a numerical technique is useful for the observation of a single diffraction process assuming illumination with a Gaussian

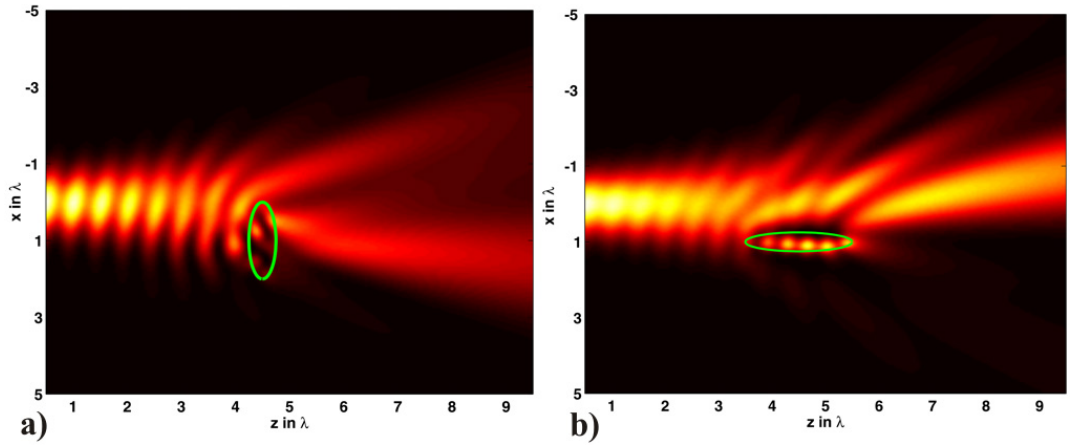

Figure 7. Intensity distribution upon illuminating an elliptical particle elongated (a) perpendicular and (b) parallel to the optical axis with a Gaussian beam.

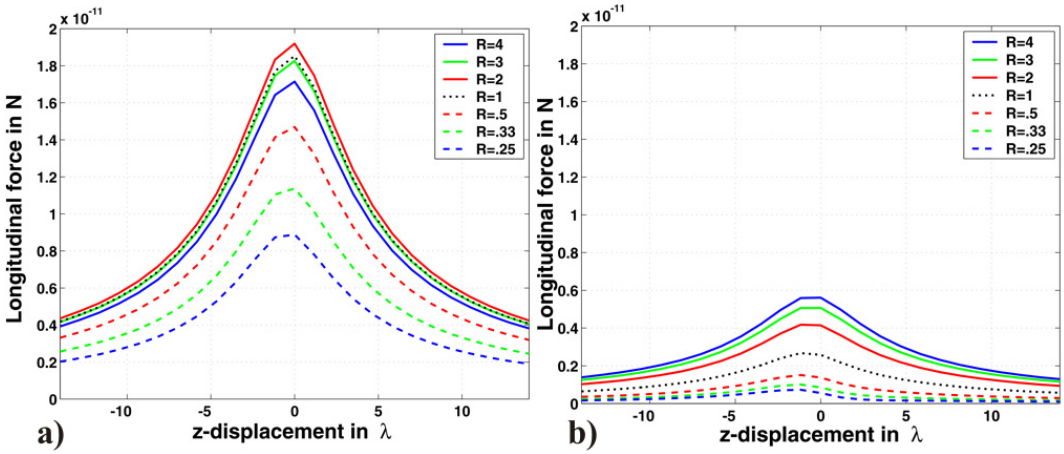

Figure 8. Longitudinal force on a dielectric elliptical cylinder on the axis with $r_{\mathrm{Ref}} = 0.1\lambda$ assuming (a) a TE-polarized and (b) a TM-polarized Gaussian beam for illumination.

beam, as the computational time is smaller compared to the MMP. A spatial discretization of $\frac{\lambda}{20}$ was used for the numerical grid and the centre of the particle was positioned at $x = -1\lambda$ relative to the beam axis and at $z = 4.5\lambda$ relative to the waist of the laser ($\omega = \lambda$). As boundaries of the computational domain, perfectly matched layers were used [35].

Figure 7(a) shows the intensity of the field when illuminating a particle elongated perpendicular and figure 7(b) for a particle elongated parallel to the optical axis. By examining the time-resolved field propagation as well as the resulting intensity distributions after the diffraction process, we see in figure 7(a) that the light hitting the first surface of the particle is refracted, and refracted once again upon exiting the other side. Because the long side of the particle is exposed to the incoming light, a large amount of light is deflected and the light which passes through the particle propagates away from the optical axis. Due to momentum conservation, as used in the ray-optical model, momentum must be transferred to the particle and the direction of the impulse, which translates to a force and points in the opposite direction to the deflected beam. This means towards the optical axis, which explains why these elliptical objects are attracted towards this axis. In contrast, in figure 7(b) a large amount of light is scattered at the surface due to the grazing incidence, since the intensity of the illuminating beam is higher on the side at the particle closest to the optical axis. The majority of the light is deflected by the structure towards the optical axis, thus pushing the particle away. Elliptical particles elongated along the optical axis are repelled if they are positioned behind the waist.

4. Small dielectric particles in air

Such a pronounced difference in the response (e.g. a different sign of the transversal force) is significantly reduced if the size of the particles is smaller. The longitudinal force on the elliptical particles with the same axis ratios but now with a reference radius of $r_{\mathrm{Ref}} = 0.1\lambda$ is shown in figure 8(a) for TE- and in figure 8(b) for TM-polarized light. All the other parameters are the same as above.

For TE-polarized light the qualitative distribution of the force that acts on the particles is nearly the same for the elongation directions. If one would plot the force normalized with respect to its maximum, all lines coincide to a good approximation. Only the strength varies, which has its maximum for the particle whose radius r_1 is divided by a factor of $\sqrt{2}$, having an ellipticity of 2. If the objects are

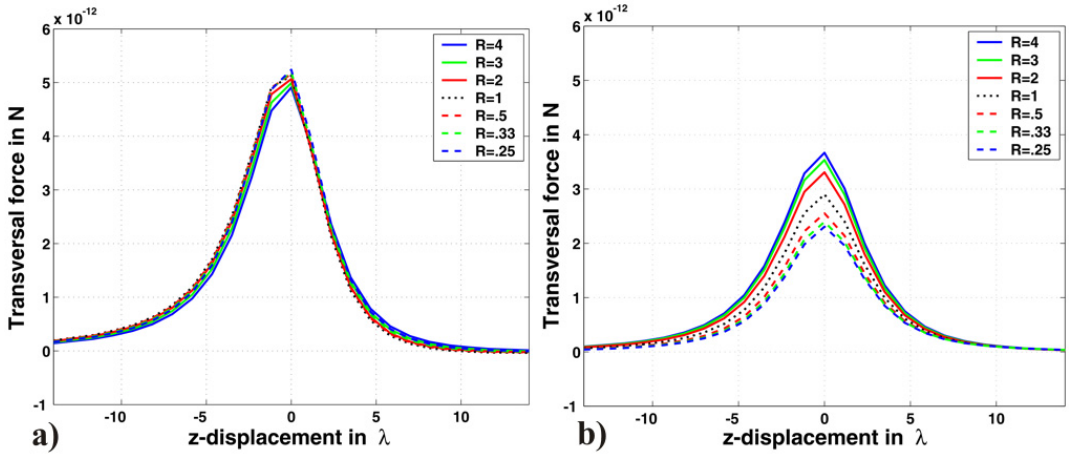

Figure 9. Transversal force along $x = -0.44\lambda$ on a dielectric elliptical cylinder with $r_{\mathrm{Ref}} = 0.1\lambda$ assuming (a) a TE-polarized and (b) a TM-polarized Gaussian beam for illumination.

illuminated with TM polarized light, the particle with the highest longitudinal force is the particle with a radius $r_1 = \frac{0.1}{\sqrt{4}}\lambda$. For a larger radius r_1, the maximum of the force is smaller. By comparing qualitatively the forces that act on the particles we see that the forces before the waist have an equal distribution independent of the particles elongation. Behind the waist, the force decreases more rapidly for an elongation in the longitudinal direction.

The reduced influence of the shape on the force can be likewise seen in figure 9(a) for TE polarization and in figure 9(b) for TM polarization, where the transversal force along the line $x = -0.44\lambda$ is shown. It can be seen that the force for the TE-polarized Gaussian beam illumination is the same, regardless of the elongation direction. Comparing the results for TE with those of TM polarization we see a difference, because the forces acting on the differently elongated particles are different in strength for TM polarization. This effect is attributed to the dominance of a dipole excitation within the structure and will be more pronounced for much smaller particles.

Comparing the transversal and longitudinal forces we see that the strength for the transversal force is approximately a quarter of the strength of the longitudinal force for TE polarization and only half for TM polarization. In both cases this means that the particle is pushed towards the optical axis.

A further reduction of the particle size will reduce the dominance of the scattering force component and will hence enhance the influence of the gradient force acting on the particle. As outlined in the introduction, the particles can be described by a simple dipole model and the force acting on the object can be decomposed into a gradient and scattering force. The gradient force will point towards the gradient of the square of the absolute value of the electric-field. For a spherical cylinder the z-component of the gradient force along the axis will equal at a certain radius the z-component of the scattering force. If such a condition is fulfilled, a point exists in space with a net force acting on the particle equal to zero. This is a point in which the particle can be trapped. Assuming TE-polarization, the necessary radius for the particle to be trapped is $r = 0.018\lambda$. For TM polarization the radius is nearly twice as large, $r = 0.034\lambda$. For the parameters used throughout the text the particle is stably trapped at $z = 2.9\lambda$.

5. Dielectric particles much smaller than the wavelength in air

For particles smaller than this critical radius the longitudinal force along the optical axis has two points where it is zero. But only at one point that is closer to the waist can the particle be trapped stably. The other point is unstable.

Figure 10(a) shows the longitudinal force acting on the elliptical particles with a reference radius of $r_{\mathrm{Ref}} = 0.01\lambda$ for TE-polarized light and in figure 10(b) for TM-polarized light. It can be seen that the longitudinal force that acts on the particle becomes independent of the elongation direction for TE polarization. For TM polarization the longitudinal force has a constant ratio, which depends on the axis ratio.

For an explanation of this different behaviour, we derive the longitudinal force on an elliptical cylinder in the quasi-static limit for the two polarizations. We will restrict ourselves to plane wave illumination because this is sufficient to explain the different behaviour.

In this case the longitudinal force is equal to the scattering force, because the gradient of the square of the absolute value of the electric field is zero. The scattering force is given by [7]

$$F_{\mathrm{sca}}(\mathbf{r}) = \frac{C_{\mathrm{sca}}\langle \mathbf{S}(\mathbf{r},t)\rangle_T}{c/n_a} = \hat{z}\left(\frac{n_a}{c}\right) C_{\mathrm{sca}}\mathbf{I}(\mathbf{r}). \qquad (4)$$

$\mathbf{I}$ is the intensity, c is the speed of light in vacuum, $\mathbf{S}$ is the Poynting vector and C_{sca} is the scattering cross section.

The scattering cross section for an ellipsoid with the semi-axes r_1, r_2 and r_3 approximation is given by in the dipole [36]

$$C_{\mathrm{sca}} = \frac{k^4}{6\pi}|\alpha_i|^2, \qquad (5)$$

with α_i being the polarizability for the axis i. It is defined as [36]

$$\alpha_i = 4\pi r_1 r_2 r_3 \frac{\epsilon_{\mathrm{p}} - \epsilon_{\mathrm{s}}}{3\epsilon_{\mathrm{s}} + 3L_i(\epsilon_{\mathrm{p}} - \epsilon_{\mathrm{s}})} \qquad i = 1, 2, 3. \qquad (6)$$

ϵ_{p} and ϵ_{s} are the dielectric constants of the particle and of the surrounding medium, respectively. L_i is the so-called

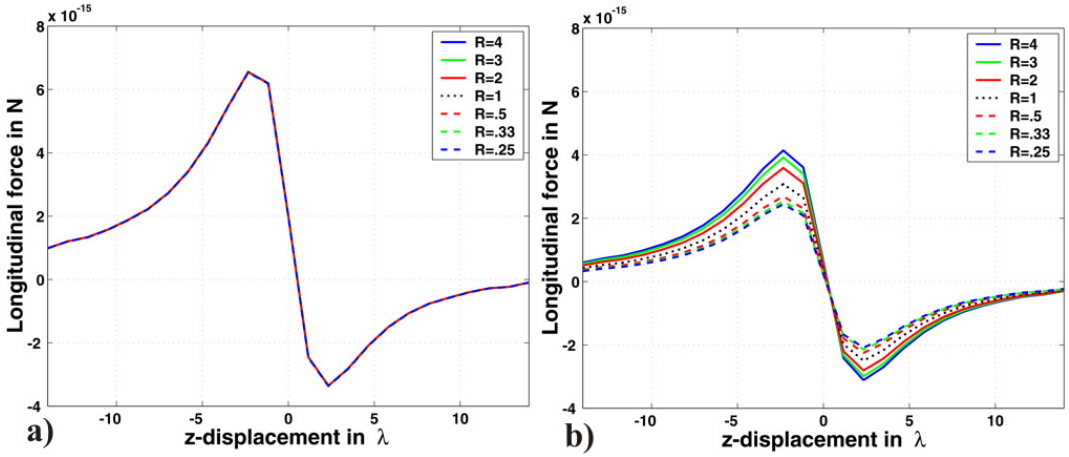

Figure 10. Longitudinal force on a dielectric elliptical cylinder on the axis with $r_{\mathrm{Ref}} = 0.01\lambda$ assuming (a) a TE-polarized and (b) a TM-polarized Gaussian beam for illumination.

geometrical factor and is defined as

$$L_i = \frac{r_1 r_2 r_3}{2} \int_0^\infty \frac{\mathrm{d}s}{(s + r_i^2) f(s)}, \tag{7}$$

with

$$f(s) = \sqrt{(s + r_1^2)(s + r_2^2)(s + r_3^2)}. \tag{8}$$

In the limit of a cylindrical structure, one of the three radii tends to infinity. In the case of TE polarization, the field oscillates parallel to this radius (the cylinder axis) and the geometrical factor becomes zero independent of the ratio of the two other axes. For TM-polarized light the electric field oscillates along the elliptical cross section of the structure. In the limit of an infinite third radius the geometrical factor L_i becomes $\frac{1}{1+R}$ for the first axis and $\frac{R}{1+R}$ for the second axis.

For TE polarization the polarizability becomes independent of the axis ratio

$$\alpha = V \frac{\epsilon_\mathrm{p} - \epsilon_\mathrm{s}}{\epsilon_\mathrm{s}}, \tag{9}$$

with V being the volume. In TM polarization the polarizability becomes

$$\alpha = V \frac{(\epsilon_\mathrm{p} - \epsilon_\mathrm{s})(1 + R)}{R\epsilon_\mathrm{s} + \epsilon_\mathrm{p}}. \tag{10}$$

Figure 11 shows the normalized longitudinal force on elliptical particles with different axis ratios and different sizes. The particles have been illuminated with a TM-polarized plane wave. Additionally, the force as evaluated with the equation (4) is shown. It can be seen that the force that acts on the particle for smaller sizes converges quite well to the force calculated using the dipole approximation.

For more complex wave fields the gradient force has to be taken into account. This force component in the dipole approximation can be calculated using [9] as

$$F_{\mathrm{grad}} = \tfrac{1}{4} n_a \alpha \,\mathrm{grad}(|E|^2). \tag{11}$$

The dependence on the polarizability indicates that the gradient force becomes independent of the elongation of the particles for TE polarization and the force will become a fixed ratio that depends on the axis ratio for TM polarization. This can

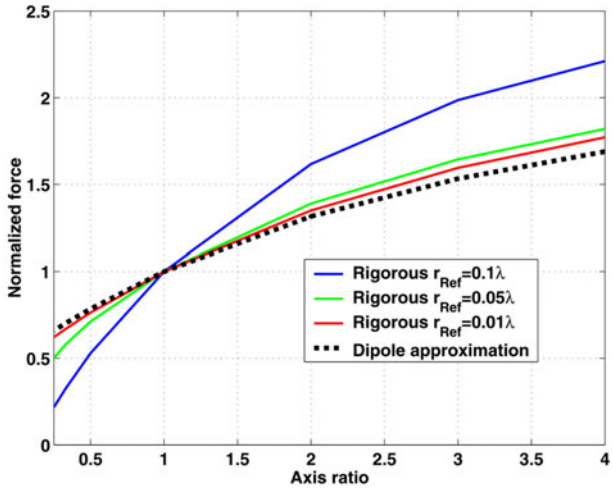

Figure 11. Normalized force on elliptical particles for plane wave illumination (TM polarization).

be seen in the calculation of the transversal force. This force depends only on the gradient force. Figure 12(a) shows the force evaluated along $x = -0.44\lambda$ for TE polarization and figure 12(b) for TM polarization, for a reference radius of $r_{\mathrm{Ref}} = 0.01\lambda$. All the other parameters are the same. The force is strongest at the spatial point with the highest gradient of the field, in the waist, and is always positive. This means that these particles are always attracted towards the optical axis.

For completeness, figure 13 shows the entire force that acts on a circular cylinder with a radius of $r = 0.01\lambda$ assuming TE-polarized light for the illumination. The force is shown on a non-linear scale to emphasize the direction. The amplitude of the illuminating beam is also included as the colour scale to the figure. It can be seen that in this size regime the gradient force is dominant over the scattering force. The contribution of the scattering force is negligible and the force is to a good approximation equal to the gradient of the square of the absolute value of the E-field.

Even though all the calculations have been done with a high index contrast, the basic effects and different interaction regimes remain essentially the same for a lower index contrast.

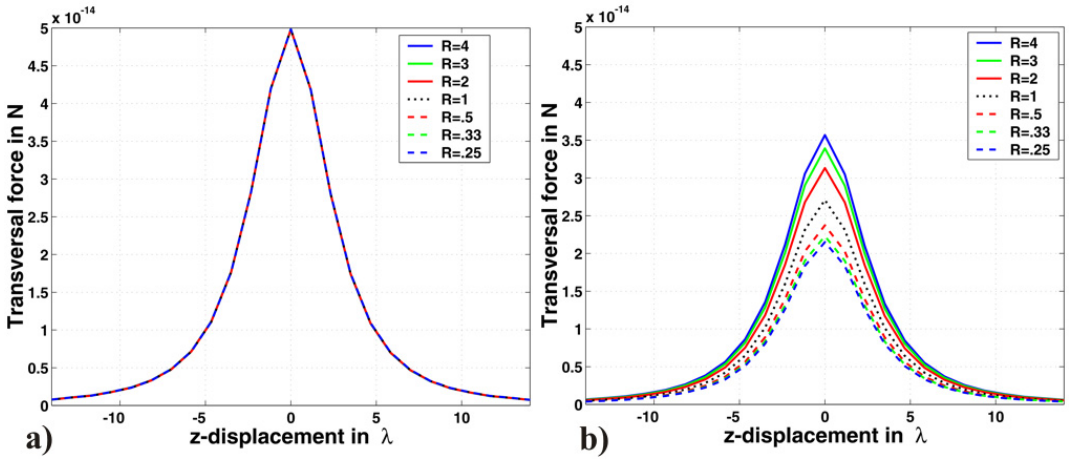

Figure 12. Transversal force along $x = -0.44\lambda$ on a dielectric elliptical cylinder with $r_{\mathrm{Ref}} = 0.01\lambda$ assuming (a) a TE-polarized and (b) a TM-polarized Gaussian beam for illumination.

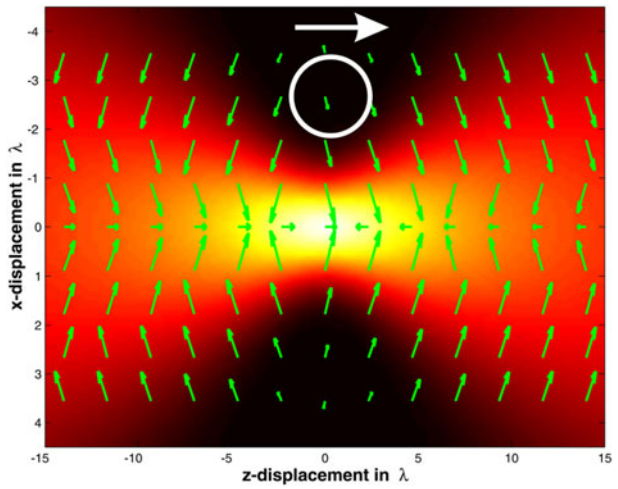

Figure 13. Force acting on a dielectric circular cylinder with $r = 0.01\lambda$ for TE polarization.

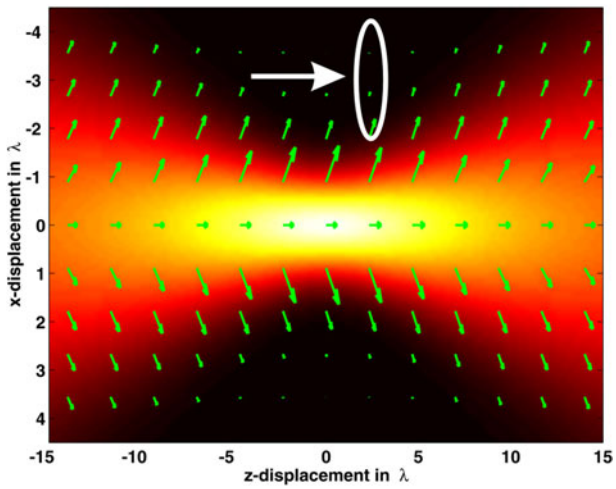

Figure 14. Force acting on a dielectric elliptical cylinder, transversally elongated ($r_1 = \frac{0.5}{\sqrt{4}}\lambda$) with $n_a = 1.5$.

The only difference at an index contrast close to unity is that the dipole approximation is valid for larger geometrical radii.

If the index contrast is lower than unity, meaning that the refractive index of the surrounding medium is larger than the index of the cylinder, a different behaviour is observed. In an experiment this situation corresponds to, e.g., air bubbles in a liquid. This case will be investigated in the next section.

6. Particles with an index contrast lower than unity

In this section we will assume an index of 1.5 for the surrounding medium and an index of 1 for the medium of the cylinder. All the other parameters remain the same. The waist remains equal to a single wavelength in vacuum. In figure 14 is shown the entire force distribution for a particle elongated perpendicular to the optical axis and whose reference radius is $r_{\mathrm{Ref}} = 0.5\lambda$. This means $r_1 = \frac{0.5\lambda}{\sqrt{4}}$. The amplitude of the illuminating beam has been added to the figure, the polarization is TE and the force is shown on a non-linear scale. It can be seen that the force acting on such a particle will always repel it from the axis if it is elongated transversally. The effect is well known and can be explained in a simple manner by analysing the polarizability α in such a configuration. The terms $(\epsilon_{\mathrm{p}} - \epsilon_{\mathrm{s}})$ and α take negative values. Consequently, the gradient force is negative and points away from the optical axis. For the calculation of the scattering force, the absolute value of α is taken into account and the force is consequently positive, pointing in the propagation direction of the beam.

Figure 15 shows the entire force distribution for an elliptical particle elongated parallel to the optical axis, thus $r_1 = 0.5\lambda\sqrt{4}$. Only for such highly elongated particles in the longitudinal direction, the particles are attracted towards the optical axis when it is placed before the waist of the beam. In a similar manner to the explanation in the last section, for such a highly longitudinally elongated particle, the deflection rather than refraction of the laser beam at the elongated surface will lead to a propagation of the beam away from the optical axis. Due to conservation of momentum, the particle is pushed towards the axis. The basic behaviour of these particles is exactly the same as we have analysed already for the dielectric particles in air. The difference is the opposite sign of the

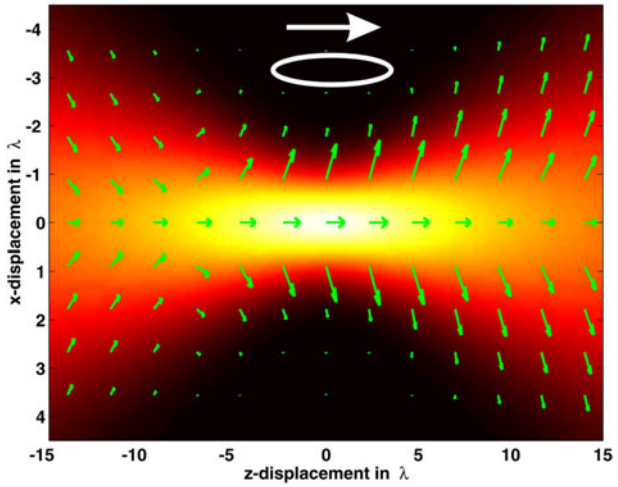

Figure 15. Force acting on a dielectric elliptical cylinder, longitudinally elongated ($r_1 = 0.5\sqrt{4}\lambda$) with $n_a = 1.5$.

transversal force and the corresponding opposite behaviour of attraction and repulsion when placing it before or behind the laser beam.

A point of stable trapping in 3D for such a configuration is not possible. The on-axis longitudinal force may be negative if the particle is sufficiently small, but the transversal force will always push the particle away from the optical axis, hence there are only unstable points on the optical axis. In figure 16(a) the longitudinal force along the axis for particles with different elongations is shown for TE polarization and in figure 16(b) for TM polarization. The reference radius of the elliptical cylinder is $r_{\mathrm{Ref}} = 0.01\lambda$. It can be seen that the force becomes independent of the elongation for TE-polarized light, as suggested by the calculated polarizability using equation (9). The force has its maximum at a position somewhat behind the waist.

On the other hand the force on the particle for a TM-polarized wave depends on the shape because the polarizability is shape-dependent as given by equation (10). The force is strongest for particles elongated in the longitudinal direction. The radius r_1 of this particle is $r_1 = 0.01\sqrt{4}$. Such a tendency is confirmed by using the dipole model.

For completeness we show in figures 17(a) and in (b) the transversal force that acts on the particle elongated parallel to the optical axis at $x = -0.44\lambda$ for TE polarization and for TM polarization, respectively. The force is negative, which means that the particles are repelled from the optical axis. For TE polarization the force is independent of the particle elongation.

If the aim is to attract these particles towards the optical axis, it is well known that higher-order Gauss–Laguerre modes in 3D and Gauss–Hermite modes in 2D can be used [6, 37]. The decomposition of the illuminating beam into a plane wave spectrum in the computational procedure, permits an efficient evaluation of the response of the structure to different illumination beams. In figure 18 we show the force that acts on an circular cylinder with a radius of $r = 0.5\lambda$ with a Gauss–Hermite beam of order 1. The force is shown again on a non-linear scale to emphasize the direction. It can be seen that the particle will react to the local gradient of the field, which pushes the particle towards the optical axis as long as it is spatially confined to the central part of the beam.

7. Conclusions

In this paper applied rigorous methods for the investigation the force on dielectric elliptical cylinders as a function of the elongation direction within different size domains. We have analysed the behaviour for different index contrasts.

It has been shown that geometrically large elliptical particles with an index contrast larger than unity and elongated in the transversal direction are always attracted towards the optical axis, whereas particles elongated in the longitudinal direction are attracted if they are positioned before the waist of the laser beam and repelled if positioned after the waist. An explanation was given by analysing the process of the interaction, which is dominated in the different regimes by either refraction or reflection, depending on the elongation direction of the particle relative to the optical axis.

If the particles are much smaller than the wavelength, the force can be decomposed assuming a dipole model into a

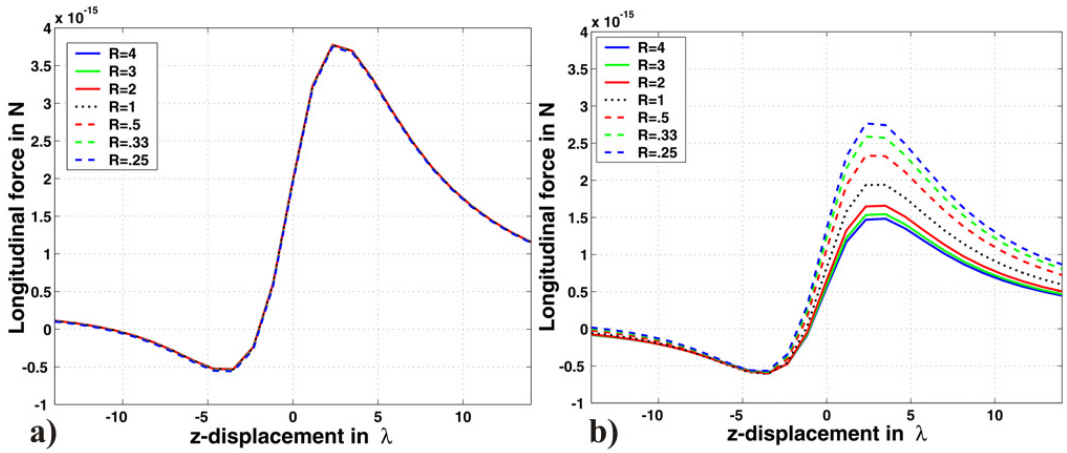

Figure 16. Longitudinal force on a dielectric elliptical cylinder on the axis with $r_{\mathrm{Ref}} = 0.01\lambda$ assuming (a) a TE-polarized and (b) a TM-polarized Gaussian beam for illumination with $n_a = 1.5$.

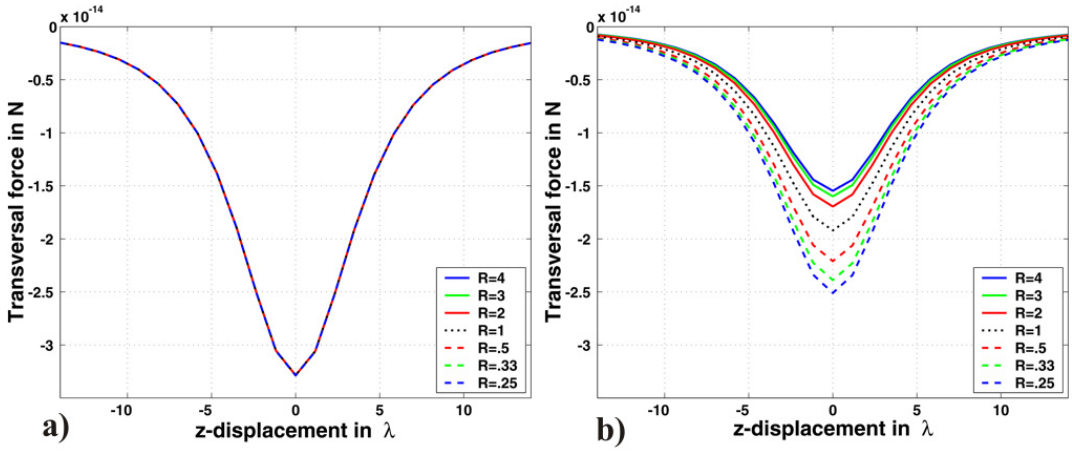

Figure 17. Transversal force along $x = -0.44\lambda$ on a dielectric elliptical cylinder with $r_{\mathrm{Ref}} = 0.01\lambda$ assuming (a) a TE-polarized and (b) a TM-polarized Gaussian beam for illumination with $n_a = 1.5$.

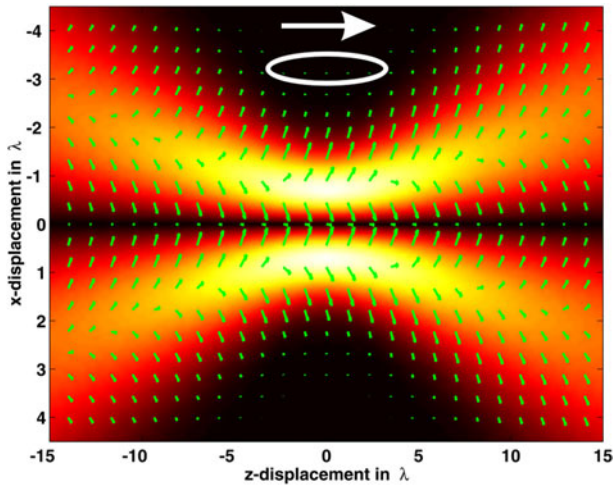

Figure 18. Force acting on a longitudinally elongated dielectric elliptical cylinder ($r_1 = 0.5\sqrt{4}\lambda$) with $n_a = 1.5$, illuminated with a GH1 beam.

scattering component which points in the propagation direction of the laser beam and a gradient force. The gradient force points towards the gradient of the square of the absolute value of the electric field. For a Gaussian beam this force will point towards the waist. If the z-component of the gradient force equals the scattering force, stable trapping in three dimensions becomes possible. By using the dipole model as well as our rigorous simulations, it was shown that for TE-polarized light the force becomes independent of the elongation. In contrast, for the TM polarization the force will converge towards a fixed ratio that depends on the axis ratio.

Similar investigations have been made for systems with an index contrast lower than unity. In these systems the sign of the gradient force is negative. The gradient force hence will point in the opposite direction to the gradient of the field. This results in a repulsion from the optical axis for large transversal elongated particles independent of their position relative to the waist. Longitudinally elongated particles can be attracted if they are positioned before the waist, otherwise they are likewise repelled. For particles much smaller than the wavelength the same dependence of the response as a function of the polarization was found as for dielectric particles in air. For TE-polarized light the force does not depend on the elongation, whereas for TM polarization it does. These particles cannot be stably trapped because the gradient force will always point away from the optical axis. For an on-axis trapping it is necessary to use higher order Gauss–Hermite laser modes, as we have shown numerically.

The differing response of particles with different ellipticities, allows the potential application of sorting particles as a function of their shape. For example it is still problematic to fabricate particles with a controlled axis ratio, while statistical approaches such as irradiation with pulsed laser beams to deform particles yield a mixture of particles with different shapes. In this situation, the application of a sorting mechanism with optical tweezers could be a promising technique to obtain particles with a well controlled shape [38].

Acknowledgments

This research was supported by the European Union within the framework of the Future and Emerging Technologies-SLAM program under grant no IST-2000-26479.

References

[1] Ashkin A 1970 *Phys. Rev. Lett.* **24** 156
[2] Ashkin A and Dziedzic J M 1971 *Appl. Phys. Lett.* **19** 283
[3] Grier D G 2003 *Nature* **424** 810
[4] Ashkin A 1997 *Proc. Natl Acad. Sci. USA* **94** 4853
[5] Ashkin A, Dziedzic J M, Bjorkholm J E and Chu S 1986 *Opt. Lett.* **11** 288
[6] Gahagan K T and Swartzlander G A Jr 1998 *J. Opt. Soc. Am.* B **15** 524
[7] Harada Y and Asakura T 1996 *Opt. Commun.* **124** 529
[8] Lewittes M, Arnold S and Oster G 1982 *Appl. Phys. Lett.* **40** 455
[9] Kawata S, Inouye Y and Sugiura T 1994 *Japan. J. Appl. Phys.* **33** L1725
[10] Arias-Gonzáles J R and Nieto-Vesperinas M 2003 *J. Opt. Soc. Am.* A **20** 1201
[11] Nieminen T A, Rubinsztein-Dunlop H, Heckenberg N R and Bishop A I 2001 *Comput. Phys. Commun.* **142** 468
[12] Gouesbet G and Gréhan G 2000 *Atomization Sprays* **10** 277

[13] Gouesbet G, Maheu B and Gréhan G 1980 *J. Opt. Soc. Am.* A **5** 1427
[14] Barton J P, Alexander D R and Schaub S A 1989 *J. Appl. Phys.* **66** 4594
[15] Onofri F, Grehan G and Gouesbet G 1980 *J. Opt. Soc. Am.* A **34** 7113
[16] Mees L, Ren K F, Gréhan G and Gouesbet G 1999 *Appl. Opt.* **38** 1867
[17] Gouesbet G and Mees L 1999 *J. Opt. Soc. Am.* A **16** 1333
[18] Ren K F, Gréhan G and Gouesbet G 1999 *Opt. Commun.* **108** 343
[19] Lock J A 2004 *Appl. Opt.* **43** 2532
[20] Lock J A 2004 *Appl. Opt.* **43** 2544
[21] Polaert H, Gréhan G and Gouesbet G 1998 *Opt. Commun.* **155** 169
[22] Bayoudh S, Nieminen T A, Heckenberg N R and Rubinsztein-Dunlop H 2003 *J. Mod. Opt.* **50** 1581
[23] Chaumet P C and Nieto-Vesperinas M 2000 *Phys. Rev.* B **61** 14119
[24] Prather D W, Mirotznik M S and Mait J N 1997 *J. Opt. Soc. Am.* A **14** 34
[25] Rockstuhl C, Salt M and Herzig H P 2003 *J. Opt. Soc. Am.* A **20** 1969
[26] Hafner C 1999 *Post-Modern Electromagnetics* (New York: Wiley)
[27] Saleh B and Teich M 1991 *Fundamentals of Photonics* (New York: Wiley)
[28] Jackson J D 1975 *Classical Electrodynamics* (New York: Wiley)
[29] Wang X, Wang X B and Cascoyne P R C 1997 *J. Electrost.* **39** 277
[30] Lester M and Nieto-Vesperinas M 1999 *Opt. Lett.* **24** 936
[31] Moreno E, Erni D E, Hafner C and Vahldieck R 2002 *J. Opt. Soc. Am.* A **19** 101
[32] Hafner C 1990 *The Generalized Multipole Technique for Computational Electromagnetics* (Boston, MA: Artech House Books)
[33] Mie G 1908 *Ann. Phys., Lpz.* **25** 377
[34] Taflove A and Hagness S C 2000 *Computational Electrodynamics* (Boston, MA: Artech House Publishers)
[35] Berenger J P 1994 *J. Comput. Phys.* **114** 185
[36] Wang D, Guo S, Ren H and Yin S 2002 *Opt. Lett.* **27** 992
[37] He H, Heckenberg N R and Rubinsztein-Dunlop H 1995 *J. Mod. Opt.* **42** 217
[38] MacDonald M P, Spalding G C and Dholakia K 2003 *Nature* **426** 421